Static Deformation Caused by a Tensile Fault Embedded in an Isotropic Half-Space Perfectly Joined with an Orthotropic Half-Space

Sangeeta [1], Meenal Malik [2], J.S. Sikka [3]

[1, 3] Department of Mathematics, Maharshi Dayanand University, Rohtak, India

[2] All India Jat Heroes' Memorial College, Rohtak, India

Email: [1] ssangeeta1529@gmail.com, [2] meenaljalaj@gmail.com, [3] sikkajs@yahoo.in

Abstract

An analytical model is proposed to determine the static response of two perfectly joined homogeneous elastic half-spaces, lower half-space is taken as orthotropic which is in welded contact with upper half-space taken as isotropic. Analytical expressions for stresses caused by a tensile dislocation embedded in the isotropic half-space are obtained. The integral expressions for the stress field are obtained by the usage of Airy stress function. Variations of the stresses with the epicentral distance for various source locations embedded in the upper half-space are discussed with the help of 2-D and 3-D graphics. We have taken the lower half-space as Topaz and Barytes for graphical representation. Numerical computations indicate that the stress field in this model may differ substantially from the stress field when both the half-spaces are isotropic.

Index Terms—Deformation, Stresses, Tensile fault, Welded contact.

1. Introduction

Seismology is the scientific study of the occurrence of earthquakes and the passage of seismic waves through the Earth. To examine the deformation fields of the medium due to earthquake faults, static dislocation earth models are used. Modeling of deformation fields due to dyke injection in the volcanic zone, mine collapse, and fluid deriven cracks are some of the important geophysical applications of the tensile fault representation model.

Seismic dislocation theory is the study of the relationship between seismic fault slip and geophysical field change. It is also the link between the source mechanism, the inner structure of the Earth, earthquake forecasting, and other fundamental geophysical problems. Due to the geometric difficulty of the commonly used dislocation theory of the semi-infinite medium model, it is riskily possible to apply seismic deformation and geodynamics analysis with some degree of oversight or even fault.

Many researchers have investigated the deformation of various earth models caused by 2-D sources. References [1] and [2] used the elastic theory of dislocations to solve the deformation field induced by a strike-slip fault with uniform slip for a 3-D model. Reference [3] derived expressions for the displacement field and stress field for a semi-infinite Poisson solid caused by vertical and horizontal tensile faults. Reference [4] considered the plane strain problem for the representation of 2-D seismic sources in an unbounded medium to obtain the Airy stress function and various source coefficients. Reference [5] discussed the static deformation of an orthotropic multilayered half-space due to normal and shear line loads by using the transfer matrix approach. Reference [6] derived the analytical expressions for the deformation fields of a two-phase (isotropic and orthotropic) model due to 2-D seismic sources.

Reference [7] studied the problem of a uniform half-space with traction free surface produced by a vertical tensile fault. The closed form analytical expressions for Airy stress function for two media in smooth contact induced by a vertical tensile fault has been investigated by [8]. In an elastic medium, the effect of irregularity and initial stresses for the normal and tangential loading has been observed by [9]. Stress field for two (isotropic and orthotropic) perfectly joined half-spaces caused by a dip-slip fault embedded in the isotropic half-space obtained by [10]. Numerical results were discussed by using dimensionless approach with the help of 2-D and 3-D mesh grids. As an orthotropic materials Topaz and Barytes are taken for graphical representation.

Our main aim of this paper is to mathematically analyse the plane strain deformation induced by a horizontal and a vertical tensile fault embedded in an isotropic half-space perfectly joined with an orthotropic elastic half-space. Following the results of [6] we have investigated variations of the stress field with distance from the fault and distance from the interface produced by a tensile fault using 2-D and 3-D graphics.

2. Theory

Let the Cartesian co-ordinate system be denoted by (x, y, z) with z-axis vertically upwards. Two homogeneous elastic half-spaces are taken into welded contact at the interface $z = 0$. Upper half-space $(z > 0)$ is taken as isotropic (medium I) and lower half-space $(z < 0)$ is taken as orthotropic (medium II). A 2-D approximation is considered in which the displacement components (u_1, u_2, u_3) are independent of x so that $\partial/\partial x \equiv 0$. For a line dislocation passing through the point $(0,0,h)$ in medium I, the Airy stress function for medium I and II are given by [6]

$$U^{(\mathrm{I})} = U_0 + \int_0^\infty [(L_1 + M_1 kz)\sin ky + (P_1 + Q_1 kz)\cos ky] e^{-kz} k^{-1} dk \quad (1)$$

$$U^{(\mathrm{II})} = \int_0^\infty [(L_2 e^{akz} + M_2 e^{bkz})\sin ky + (P_2 e^{akz} + Q_2 e^{bkz})\cos ky] k^{-1} dk \quad (2)$$

where

$$U_0 = \int_0^\infty [(L_0 + M_0 k|z-h|)\sin ky + (P_0 + Q_0 k|z-h|)\cos ky] k^{-1} e^{-k|z-h|} dk \quad (3)$$

$$a^2 + b^2 = (c_{22}c_{33} - c_{23}^2 - 2c_{23}c_{44})/(c_{33}c_{44}),$$
$$a^2 b^2 = c_{22}/c_{33} \quad (4)$$

Values of constants L_1, M_1 etc. are to be determined from the boundary conditions and are given by [6]

$$L_1 = [X_1(L^- + M^- kh) + 2(D - C)M^-]e^{-kh},$$

$L_2 = [2A(L^- + M^- kh) - 2CM^-]e^{-kh}$
$M_1 = [2X_2(L^- + M^- kh) + X_3M^-]e^{-kh},$
$M_2 = [2B(L^- + M^- kh) + 2DM^-]e^{-kh}$
$P_1 = [X_1(P^- + Q^- kh) + 2(D - C)Q^-]e^{-kh},$
$P_2 = [2A(P^- + Q^- kh) - 2CQ^-]e^{-kh}$
$Q_1 = [2X_2(P^- + Q^- kh) + X_3Q^-]e^{-kh},$
$Q_2 = [2B(P^- + Q^- kh) + 2DQ^-]e^{-kh}$ (5)

where h is the source depth and L^-, M^-, P^-, Q^- are the values of L_0, M_0, P_0, Q_0 for $z < h$, and

$X_1 = 2(A + B) - 1,$
$X_2 = A(1 + a) + B(1 + b) - 1,$
$X_3 = 2D(1 + b) - 2C(1 + a) + 1$
$A = \alpha_1(1 - b + 2\mu_1 s_2 - 2\mu_1 r_2)/W,$
$B = \alpha_1(a - 1 + 2\mu_1 r_1 - 2\mu_1 s_1)/W$
$C = (1 + b - b\alpha_1 + 2\mu_1\alpha_1 s_2)/W,$
$D = (1 + a - a\alpha_1 + 2\mu_1\alpha_1 s_1)/W,$
$W = (1 + a - \alpha_1 + 2\mu_1\alpha_1 r_1)(1 + b - b\alpha_1 + 2\mu_1\alpha_1 s_2)$
$\quad -(1 + a - a\alpha_1 + 2\mu_1\alpha_1 s_1)(1 + b - \alpha_1 + 2\mu_1\alpha_1 r_2),$
$\alpha_1 = \frac{\lambda_1 + \mu_1}{\lambda_1 + 2\mu_1}$ (6)
$r_1 = (c_{33}a^2 + c_{23})/\Delta, \; r_2 = (c_{33}b^2 + c_{23})/\Delta$ (7)
$s_1 = (c_{23}a + c_{22}/a)/\Delta, \; s_2 = (c_{23}b + c_{22}/b)/\Delta$ (8)

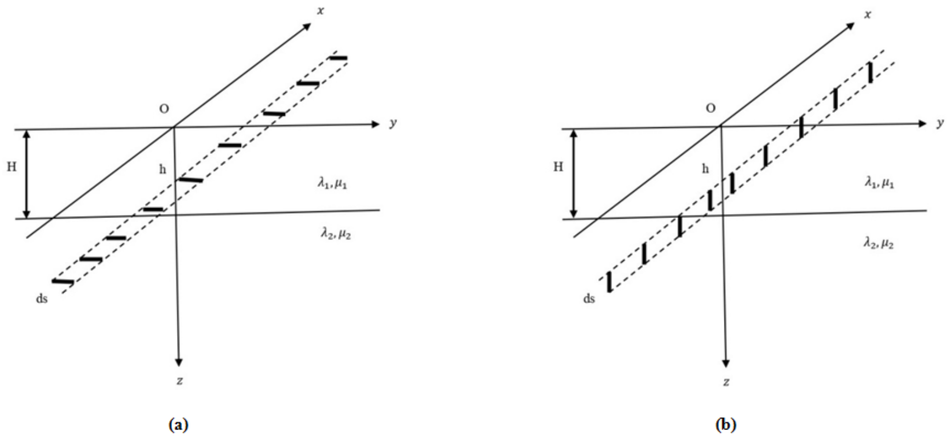

Figure 1: Geometry of a line dislocation of finite width ds and infinite length embedded in the upper half-space at the point $(0,0,h)$ representing (a) horizontal tensile fault (b) vertical tensile fault

3. Tensile Fault

Horizontal Tensile Fault. The source coefficients values are given by [6]

$L_0 = M_0 = 0, P_0 = Q_0 = \frac{\alpha_1\mu_1 bds}{\pi}$
$L^- = M^- = 0, P^- = Q^- = \frac{\alpha_1\mu_1 bds}{\pi}$

where b is the magnitude of displacement discontinuity.

Using the values of source coefficients in the expressions of stresses obtained by [6], we have

$$\tau_{22}^{(\mathrm{I})}=\frac{\alpha_1\mu_1 bds}{\pi}\left[\frac{1}{R^2}\left\{1-\frac{8(z-h)^2}{R^2}+\frac{8(z-h)^4}{R^4}\right\}\right.$$
$$+\frac{1}{S^2}\left\{4X_2-X_1-\frac{2(z+h)[6X_2z-(X_1-4X_2)(z+h)]}{S^2}+\frac{16X_2z(z+h)^3}{S^4}\right\}$$
$$+\frac{2}{S^2}\left\{X_3-D+C\right.$$
$$+\frac{(z+h)[2(D-C)(z+h)-3(X_1-4X_2)h-X_3(5z+2h)]}{S^2}$$
$$\left.\left.+\frac{6X_2hz}{S^2}+\frac{4(z+h)^3[(X_1-4X_2)h+X_3z]-48X_2hz(z+h)^2}{S^4}+\frac{48X_2hz(z+h)^4}{S^6}\right\}\right] \quad (9)$$

$$\tau_{23}^{(\mathrm{I})}=\frac{\alpha_1\mu_1 bds\,y}{\pi}\left[-\frac{2(z-h)}{R^4}\left\{-1+\frac{4(z-h)^2}{R^2}\right\}\right.$$
$$+\frac{2}{S^4}\left\{2X_2(2z+h)-X_1(z+h)-\frac{8X_2z(z+h)^2}{S^2}\right\}$$
$$+\frac{2}{S^4}\left\{(X_1-2X_2)h+X_3(2z+h)-2(D-C)(z+h)+\frac{24X_2hz(z+h)}{S^2}\right.$$
$$\left.\left.-\frac{4(z+h)^2[(X_1-2X_2)h+X_3z]}{S^2}-\frac{48X_2hz(z+h)^3}{S^4}\right\}\right] \quad (10)$$

$$\tau_{33}^{(\mathrm{I})}=\frac{\alpha_1\mu_1 bds}{\pi}\left[\frac{1}{R^2}\left\{1+\frac{4(z-h)^2}{R^2}-\frac{8(z-h)^4}{R^4}\right\}\right.$$
$$+\frac{1}{S^2}\left\{X_1-\frac{16X_2z(z+h)^3}{S^4}+\frac{2(z+h)[6X_2z-X_1(z+h)]}{S^2}\right\}$$
$$+\frac{2}{S^2}\left\{D-C-\frac{6X_2hz}{S^2}+\frac{(z+h)[3(X_1h+X_3z)-2(D-C)(z+h)]}{S^2}\right.$$
$$\left.\left.-\frac{4(z+h)^2[(X_1h+X_3z)(z+h)-12X_2hz]}{S^4}-\frac{48X_2hz(Z+h)^4}{S^6}\right\}\right] \quad (11)$$

$$\tau_{22}^{(\mathrm{II})}=\frac{2\alpha_1\mu_1 bds}{\pi}\left[-\frac{Aa^2}{T^2}+\frac{2Aa^2(h-az)^2}{T^4}-\frac{Bb^2}{H^2}+\frac{2Bb^{2(h-bz)^2}}{H^4}+\frac{Ca^2}{T^2}\right.$$
$$-\frac{2a^2(h-az)[C(h-az)+3Ah]}{T^4}$$
$$\left.+\frac{8\mathrm{Aa^2h(h-az)^3}}{\mathrm{T^6}}-\frac{\mathrm{Db^2}}{\mathrm{H^2}}+\frac{\mathrm{2b^2(h-bz)[-3Bh+D(h-bz)]}}{\mathrm{H^4}}+\frac{\mathrm{8Bb^2h(h-bz)^3}}{\mathrm{H^6}}\right] \quad (12)$$

$$\tau_{23}^{(\mathrm{II})}=\frac{4\alpha_1\mu_1 bds\,y}{\pi}\left[\frac{Aa(h-az)}{T^4}+\frac{Bb(h-bz)}{H^4}-\frac{a[Ah+C(h-az)]}{T^4}+\frac{4Aah(h-az)^2}{T^6}\right.$$

$$-\frac{b[Bh-D(h-bz)]}{H^4}+\frac{4Bbh(h-bz)^2}{H^6}\Big] \quad (13)$$

$$\tau_{33}^{(\mathrm{II})}=\frac{2\alpha_1\mu_1 bds}{\pi}\Big[\frac{A}{T^2}-\frac{2A(h-az)^2}{T^4}+\frac{B}{H^2}-\frac{2B(h-bz)^2}{H^4}-\frac{C}{T^2}+\frac{2(h-az)[3Ah+C(h-az)]}{T^4}-\frac{8Ah(h-az)^3}{T^6}+\frac{D}{H^2}+\frac{2(h-bz)[3Bh-D(h-bz)]}{H^4}-\frac{8Bh(h-bz)^3}{H^6}\Big] \quad (14)$$

Vertical Tensile Fault. The source coefficients values are given by [6]

$$L_0=M_0=0,\ P_0=\frac{\alpha_1\mu_1 bds}{\pi},\ Q_0=-\frac{\alpha_1\mu_1 bds}{\pi}$$

$$L^-=M^-=0,\ P^-=\frac{\alpha_1\mu_1 bds}{\pi},\ Q^-=-\frac{\alpha_1\mu_1 bds}{\pi}$$

Using the values of source coefficients in the expressions of stresses obtained by [6], we have

$$\tau_{22}^{(\mathrm{I})}=\frac{\alpha_1\mu_1 bds}{\pi}\Big[\frac{1}{R^2}\Big\{-3+\frac{12(z-h)^2}{R^2}-\frac{8(z-h)^4}{R^4}\Big\}+\frac{1}{S^2}\Big\{4X_2-X_1-\frac{2(z+h)[6X_2z-(X_1-4X_2)(z+h)]}{S^2}+\frac{16X_2z(z+h)^3}{S^4}\Big\}-\frac{2}{S^2}\Big\{X_3-D+C+\frac{(z+h)[2(D-C)(z+h)-3(X_1-4X_2)h-X_3(5z+2h)]}{S^2}+\frac{6X_2hz}{S^2}+\frac{4(z+h)^3[(X_1-4X_2)h+X_3z]-48X_2hz(z+h)^2}{S^4}+\frac{48X_2hz(z+h)^4}{S^6}\Big\}\Big] \quad (15)$$

$$\tau_{23}^{(\mathrm{I})}=\frac{\alpha_1\mu_1 bds\, y}{\pi}\Big[-\frac{2(z-h)}{R^4}\Big\{3-\frac{4(z-h)^2}{R^2}\Big\}+\frac{2}{S^4}\Big\{2X_2(2z+h)-X_1(z+h)-\frac{8X_2z(z+h)^2}{S^2}\Big\}-\frac{2}{S^4}\Big\{(X_1-2X_2)h+X_3(2z+h)-2(D-C)(z+h)+\frac{24X_2hz(z+h)}{S^2}-\frac{4(z+h)^2[(X_1-2X_2)h+X_3z]}{S^2}-\frac{48X_2hz(z+h)^3}{S^4}\Big\}\Big] \quad (16)$$

$$\tau_{33}^{(\mathrm{I})}=\frac{\alpha_1\mu_1 bds}{\pi}\Big[\frac{1}{R^2}\Big\{1-\frac{8(z-h)^2}{R^2}+\frac{8(z-h)^2}{R^4}\Big\}+\frac{1}{S^2}\Big\{X_1+\frac{2(z+h)[6X_2z-X_1(z+h)]}{S^2}-\frac{16X_2z(z+h)^3}{S^4}\Big\}-\frac{2}{S^2}\Big\{D-C+\frac{(z+h)[3(X_1h+X_3z)-2(D-C)(z+h)]}{S^2}-\frac{6X_2hz}{S^2}-\frac{4(z+h)^2[(X_1h+X_3z)(z+h)-12X_2hz]}{S^4}-\frac{48X_2hz(Z+h)^4}{S^6}\Big\}\Big] \quad (17)$$

$$\tau_{22}^{(\mathrm{II})}=\frac{2\alpha_1\mu_1 bds}{\pi}\Big[-\frac{Aa^2}{T^2}+\frac{2Aa^2(h-az)^2}{T^4}-\frac{Bb^2}{H^2}+\frac{2Bb^{2(h-bz)^2}}{H^4}-\frac{Ca^2}{T^2}+\frac{2a^2(h-az)[C(h-az)+3Ah]}{T^4}-\frac{8Aa^2h(h-az)^3}{T^6}+\frac{Db^2}{H^2}-\frac{2b^2(h-bz)[-3Bh+D(h-bz)]}{H^4}-\frac{8Bb^2h(h-bz)^3}{H^6}\Big] \quad (18)$$

$$\tau_{23}^{(\mathrm{II})}=\frac{4\alpha_1\mu_1 bds\, y}{\pi}\Big[\frac{Aa(h-az)}{T^4}+\frac{Bb(h-bz)}{H^4}+\frac{a[Ah+C(h-az)]}{T^4}-\frac{4Aah(h-az)^2}{T^6}+\frac{b[Bh-D(h-bz)]}{H^4}-\frac{4Bbh(h-bz)^2}{H^6}\Big] \quad (19)$$

$$\tau_{33}^{(\mathrm{II})}=\frac{2\alpha_1\mu_1 bds}{\pi}\Big[\frac{A}{T^2}-\frac{2A(h-az)^2}{T^4}+\frac{B}{H^2}-\frac{2B(h-bz)^2}{H^4}+\frac{C}{T^2}-\frac{2(h-az)[3Ah+C(h-az)]}{T^4}+\frac{8Ah(h-az)^3}{T^6}-\frac{D}{H^2}-\frac{2(h-bz)[3Bh-D(h-bz)]}{H^4}+\frac{8Bh(h-bz)^3}{H^6}\Big] \quad (20)$$

where

$$R^2=y^2+(z-h)^2,\quad S^2=y^2+(z+h)^2,\quad T^2=y^2+(h-az)^2,\quad H^2=y^2+(h-bz)^2 \quad (21)$$

4. Numerical Results And Discussion

We have investigated the stress field induced by a tensile fault embedded in the upper half-space (medium I). The upper half-space is considered to be isotropic while lower half-space is orthotropic. We have assumed medium I to be poissonian for numerical calculation, so that $\sigma_1 = 0.25$ and for medium II we have considered Barytes and Topaz as orthotropic materials. For numerical and graphical analysis values of the elastic constant are taken as

Topaz:

$c_{11} = 287$, $c_{22} = 3560$, $c_{33} = 3000$,

$c_{12} = 468$, $c_{23} = 900$, $c_{13} = 860$,

$c_{44} = 1100$, $c_{55} = 1350$, $c_{66} = 1330$

Corresponding to these constants, in terms of a unit of 10^6 grams wt./cm^2 values of a and b are

$a = 1.2992$, $b = 0.8385$.

Barytes:

$c_{11} = 970$, $c_{22} = 800$, $c_{33} = 1074$,

$c_{12} = 468$, $c_{23} = 273$, $c_{13} = 275$,

$c_{44} = 122$, $c_{55} = 293$, $c_{66} = 283$

Corresponding to these constants, in terms of a unit of 10^6 grams wt./cm^2 values of a and b are

$a = 2.3118$, $b = 0.3735$.

If lower half-space is also taken as isotropic,

$c_{11} = c_{22} = c_{33} = \frac{2\mu_2(1-\sigma_2)}{1-2\sigma_2}$, $c_{12} = c_{23} = c_{13} = \frac{2\mu_2\sigma_2}{1-2\sigma_2}$, $c_{44} = c_{55} = c_{66} = \mu_2$.

We take $\sigma_2 = 0.25$ and rigidity ratio $\frac{c_{44}}{\mu_1} = 0.5$ for calculation.

We have verified that, when we take medium II to be isotropic, results of present paper coincide with the results of [11].

Figs. 2(a) and 2(b) show variations of the normal stress (Σ_{22}) with distance from the fault induced by a horizontal tensile fault for $Z = 0.5$, 2, 3 (medium I), $Z = 0.2$ (medium II) for Topaz and Barytes respectively. We can observe that normal stress is more sensitive in case of Barytes than Topaz. The normal stress is symmetric about the line $Y = 0$ and attains maximum value at $Y = 0$.

The variation of shear stress (Σ_{23}) with distance from a horizontal tensile fault is illustrated in Figs. 3(a) and 3(b) for the lower half-space represented by Topaz and Barytes, respectively. Shear stress is anti-symmetric about the line $Y = 0$, and its magnitude is zero at $Y = 0$. In case of orthotropic medium taken as Topaz the shear stress is less sensitive than Barytes. Magnitude of shear stress decreases for isotropic medium as we move away from the interface (i.e. for large value of Z). Also as Y tends to infinity magnitude of shear stress tends to zero.

Figs. 4(a) and 4(b) depict variation of the normal stress (Σ_{33}) with distance from the fault produced by a horizontal tensile fault for $z = 0.5$, 2, 3 (medium I), $z = 0.2$ (medium II) when the orthotropic medium is Topaz and Barytes, respectively. Normal stress is symmetric about the line $Y = 0$, and its value is '0' at $Y = 0$.

In Figs. 5(a, b), 6(a, b) and 7(a, b) the deformation field induced by a horizontal tensile fault is shown by plotting 3-D mesh grid with contours.

Figs. 8(a, b), 9(a, b) and 10(a, b) display the variation of normal stress (Σ_{22}), shear stress (Σ_{23}) and normal stress (Σ_{33}) respectively with distance from the vertical tensile fault for Z = 0.5, 2, 3 (medium I), Z = 0.2 (medium II) when the lower half-space is taken as Topaz and Barytes. It can be seen that in case of Barytes all the stresses are more affected as compared to Topaz.

The stress field due to a vertical tensile fault is depicted in Figs. 11(a, b), 12(a, b) and 13(a, b) by plotting 3-D mesh grid with contours.

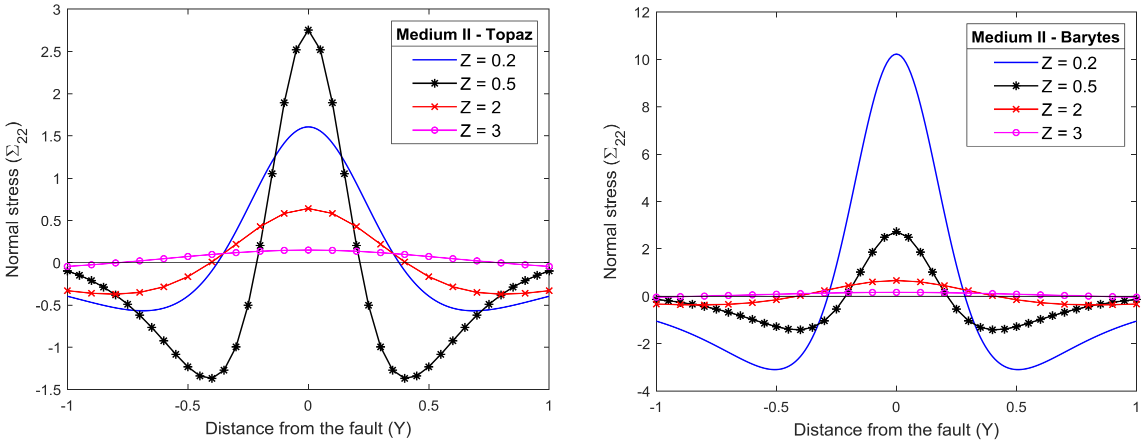

(a) **(b)**

Figure 2: Variation of the normal stress (Σ_{22}) with distance from the fault induced by a horizontal tensile fault for the orthotropic medium taken as (a) Topaz (b) Barytes

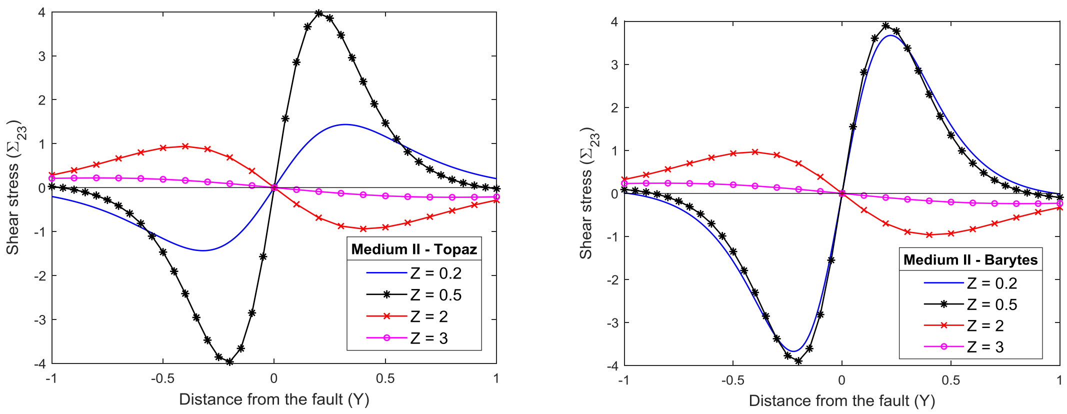

(a) **(b)**

Figure 3: Variation of the shear stress (Σ_{23}) with distance from the fault induced by a horizontal tensile fault for the orthotropic medium taken as (a) Topaz (b) Barytes

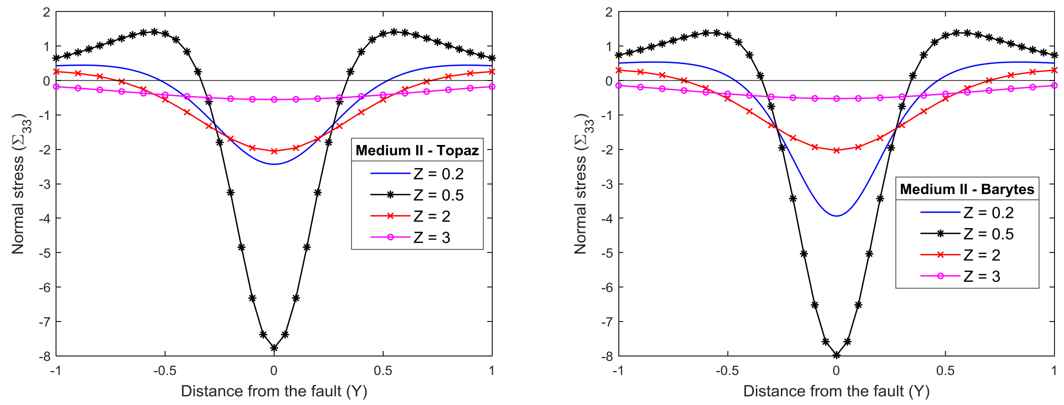

(a) **(b)**

Figure 4: Variation of the normal stress (Σ_{33}) with distance from the fault induced by a horizontal tensile fault for the orthotropic medium taken as (a) Topaz (b) Barytes

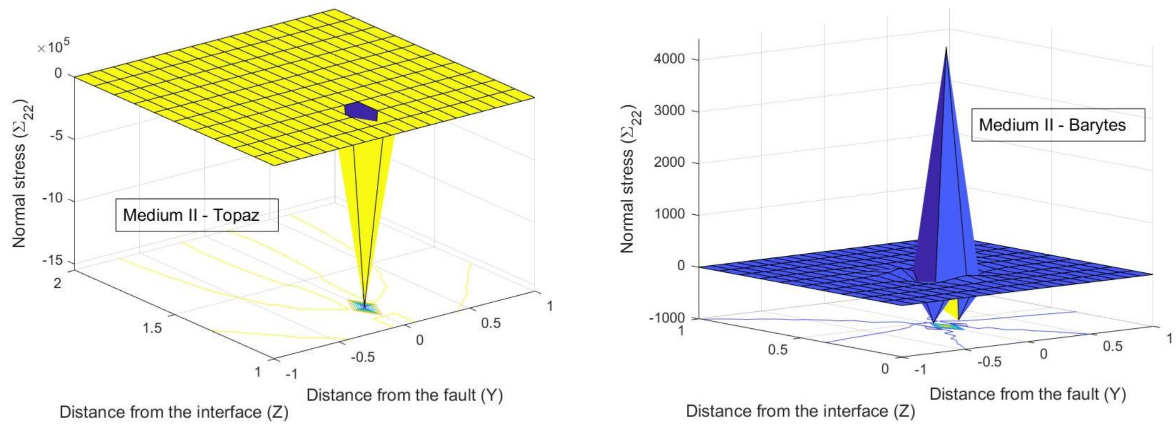

(a) **(b)**

Figure 5: 3-D mesh grid of the dimensionless normal stress (Σ_{22}) induced by a horizontal tensile fault for (a) Topaz (b) Barytes

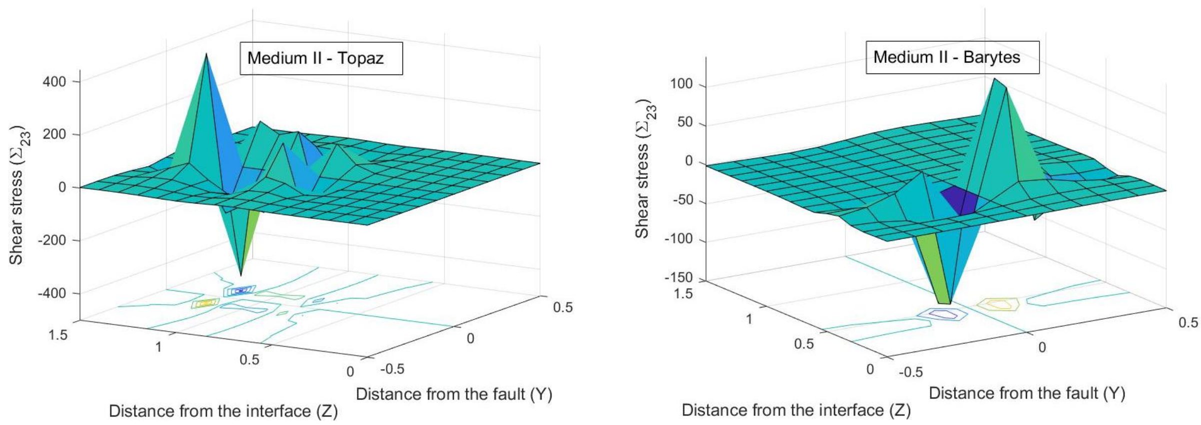

(a) **(b)**

Figure 6: 3-D mesh grid of the dimensionless shear stress (Σ_{23}) induced by a horizontal tensile fault for (a) Topaz (b) Barytes

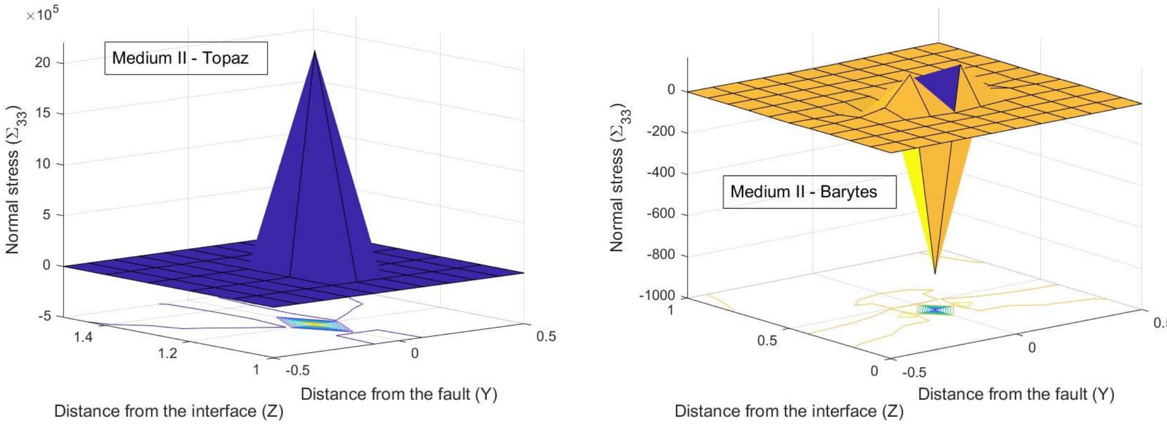

(a) **(b)**

Figure 7: 3-D mesh grid of the dimensionless normal stress (Σ_{33}) induced by a horizontal tensile fault for (a) Topaz (b) Barytes

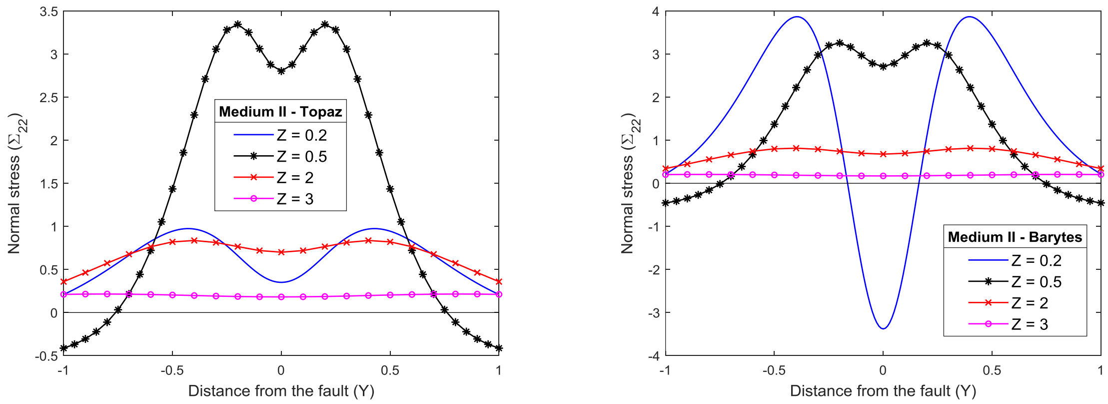

(a) **(b)**

Figure 8: Variation of the normal stress (Σ_{22}) with distance from the fault induced by a vertical tensile fault for the orthotropic medium taken as (a) Topaz (b) Barytes

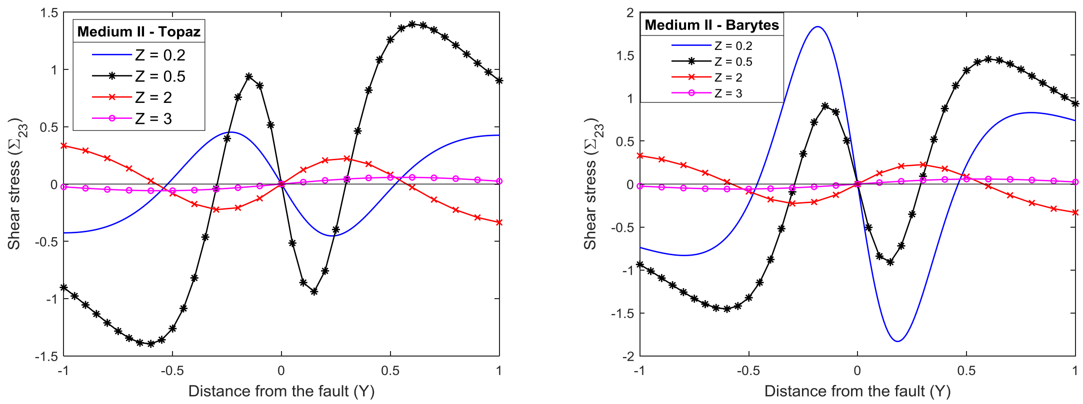

(a) **(b)**

Figure 9: Variation of the shear stress (Σ_{23}) with distance from the fault induced by a vertical tensile fault for the orthotropic medium taken as (a) Topaz (b) Barytes

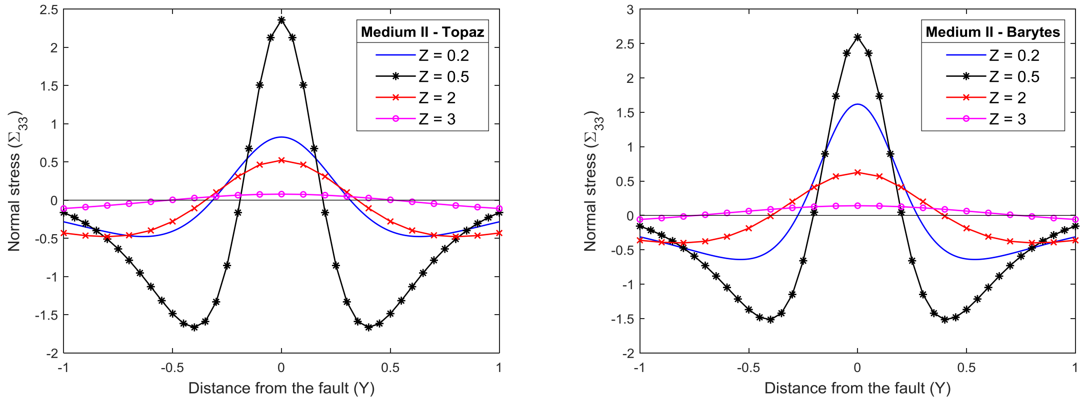

(a) **(b)**

Figure 10: Variation of the normal stress (Σ_{33}) with distance from the fault induced by a vertical tensile fault for the orthotropic medium taken as (a) Topaz (b) Barytes

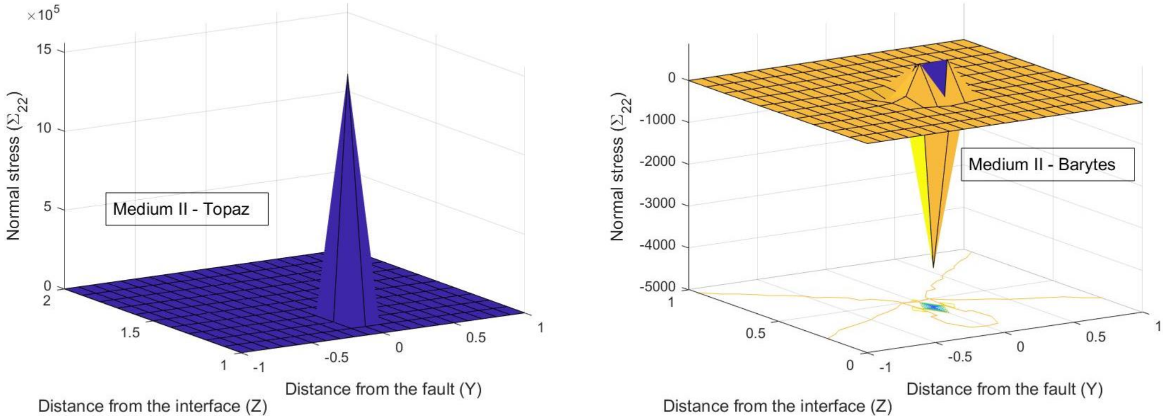

(a) **(b)**

Figure 11: 3-D mesh grid of the dimensionless normal stress (Σ_{22}) induced by a vertical tensile fault for (a) Topaz (b) Barytes

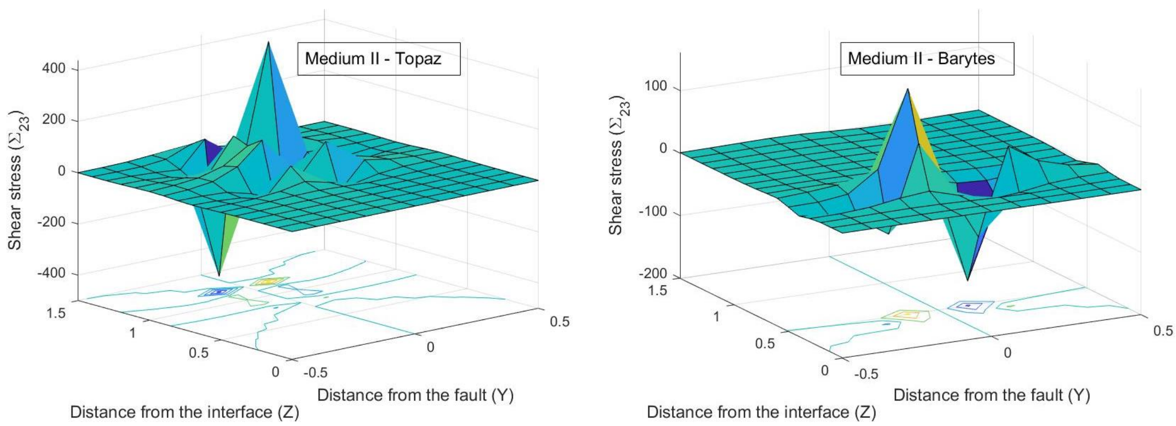

(a) **(b)**

Figure 12: 3-D mesh grid of the dimensionless shear stress (Σ_{23}) induced by a vertical tensile fault for (a) Topaz (b) Barytes

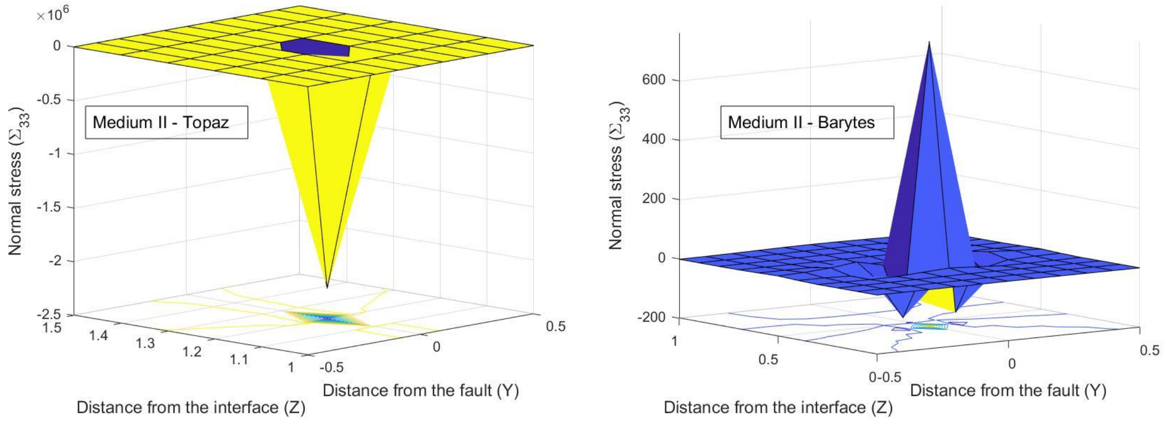

(a) **(b)**

Figure 13: 3-D mesh grid of the dimensionless normal stress (Σ_{33}) induced by a vertical tensile fault for (a) Topaz (b) Barytes

5. Conclusion

We concluded graphically that as the distance from the interface increases magnitude of the stresses decreases when the half-spaces (isotropic and orthotropic) are in welded contact. The stress field in case of Topaz is less affected in comparison to the Barytes. Also, it can be analysed that the stress field in this model may differ substantially from the stress field when both the half-spaces are isotropic.

References

[1] J. A. Steketee, "On Volterra's dislocations in a semi-infinite elastic medium," Can. J. Phys., vol. 36, pp. 192-205, 1958a.

[2] J. A. Steketee, "Some geophysical applications of the elasticity theory of dislocations," Can. J. Phys., vol. 36, pp. 1168-1198, 1958b.

[3] T. Maruyama, "Statical elastic dislocation in an infinite and semi-infinite medium," Bull. Earthq. Res. Inst., vol. 42, pp. 289-368, 1964.

[4] S. J. Singh and N. R. Garg, "On the representation of two-dimensional seismic sources," Acta Geophy. Pol., vol. 34, pp. 1-12, 1986.

[5] N. R. Garg, S. J. Singh, and S. Manchanda, "Static deformation of an orthotropic multilayered elastic half-space by two-dimensional surface loads," Proc. Indian Acad. Sci. (Earth Planet. Sci.), vol. 100, no. 2, pp. 205-218, 1991.

[6] S. J. Singh and S. Rani, "Static deformation due to two-dimensional seismic sources embedded in an isotropic half-space in welded contact with an orthotropic half-space," J. Phys. Earth, vol. 39, no. 5, pp. 599-618, 1991.

[7] M. Singh and S. J. Singh, "Static deformation of a uniform half-space due to a very long tensile fault," ISET J. Earthq. Tech., vol. 37, pp. 27-38, 2000.

[8] M. Malik, M., R. K. Sahrawat, and M. Singh, "Static deformation of two half-spaces in smooth contact due to a vertical tensile fault of finite width," IFRSA Inter. J. Comp., vol. 4, no. 1, pp. 440-450, 2014.

[9] D. K. Madan and A. Kumari, "Summerization of effect irregularity and initial stresses with normal and tangential loading in elastic medium," Inter. J. Scientific Research, vol. 5, no. 10, pp. 265-271, 2016.

[10] A. Kumari and D. K. Madan, "Stresses caused by vertical dip-slip fault embedded in an isotropic half-space joined perfectly with an orthotropic half-space," AIP Conf. Proc., vol. 2451, no. 1, pp. 1-11, 2022.

[11] S. J. Singh, S. Rani, and N. R. Garg, "Displacements and stresses in two welded half-spaces caused by two dimensional sources," Phys. Earth Plant. Int., vol. 70, pp. 90-101, 1992.